TABLE 1 Labelled structures in the optic tectum after transport of ^{125}I-labelled NT-3

Structure	Fractional area	Per cent grains 21 h	Per cent grains +TTX	Per cent grains 54 h	Labelling density 21 h	Labelling density +TTX	Labelling density 54 h
Axon	25.2	28.0	27.8	31.5	1.11	1.10	1.25
Terminal axon	9.7	10.8	12.1	6.2	1.11	1.25	0.64
Synapse	2.7	9.0	8.1	9.1	3.33	3.00	3.37
Distal dendrite	27.2	28.2	22.0	21.6	1.04	0.81	0.79
Proximal dendrite	10.3	8.8	6.6	6.2	0.85	0.64	0.60
Neuron soma	9.3	4.3	8.1	9.5	0.46	0.87	1.02
Astroglia	6.8	3.5	3.7	4.6	0.51	0.54	0.68
Unidentified	7.7	6.7	10.3	10.4	0.87	1.34	1.35
Number of grains sampled		250	130	150	–	–	–

interpretation of these data is that NT-3 is an anterogradely transported trophic messenger, although we cannot rule out an alternative interpretation, that NT-3 acts trophically on RGCs to enhance the anterograde transport and release of a second trophic factor. TTX-induced cell death was not prevented by NT-3 injected in the eye 0 or 18 h before TTX (data not shown). This suggests that TTX induces cell death by a different mechanism from PTX, and that the response to NT-3 may require activation.

Our study on the anterograde transport of exogenously introduced neurotrophins, together with recent data on the anterograde transport of endogenous neurotrophins[31], provides direct evidence that neurotrophins may act as anterograde trophic messengers. Enhanced survival may be but one of several functions of anterogradely transported neurotrophins. BDNF and NT-3 modify synaptic transmission of developing synapses[3,4], and these neurotrophins may have important functions in the stabilization of appropriate synapses and the loss of inappropriate ones during development[5,7,8]. The modification of synaptic structure and efficacy may also play a role in synaptic plasticity of the adult nervous system, and particularly in processes related to learning and memory[2]. □

Received 7 August; accepted 6 December 1995.

1. Barde, Y. A. *Neuron* **2,** 1525–1534 (1989).
2. Thoenen, H. *Trends Neurosci.* **14,** 165–170 (1991).
3. Lohof, A. M., Ip, N. Y. & Poo, M. M. *Nature* **363,** 350–353 (1993).
4. Kang, H. & Schuman, E. M. *Science* **267,** 1658–1662 (1995).
5. Purves, D. *Body and Brain. A Trophic Theory of Neural Connections* (Harvard University Press, Cambridge, 1988).
6. Cowan, W. N. in *Contemporary Research Methods in Neuroanatomy* (eds Nauta, W. J. H. & Ebbesson, S. O. E.) 217–251 (Springer, New York, 1970).
7. Changeaux, J. P. & Danchin, A. *Nature* **264,** 705–712 (1976).
8. Vaughn, J. E. *Synapse* **3,** 255–285 (1989).
9. Clarke, P. G. H. *Concepts Neurosci.* **2,** 201–219 (1991).
10. Oppenheim, R. W. *A. Rev. Neurosci.* **14,** 453–501 (1991).
11. Catsicas, M., Pequignot, Y. & Clarke, P. G. H. *J. Neurosci.* **12,** 4642–4650 (1992).
12. Korsching, S. *J. Neurosci.* **13,** 2739–2748 (1993).
13. Ferguson, I. A., Schweitzer, J. B. & Johnson, E. M. Jr *J. Neurosci.* **10,** 2176–2189 (1990).
14. Nieto-Bona, M. P., Garcia-Segura, L. M. & Torre-Aleman, I. *J. Neurosci. Res.* **36,** 520–527 (1993).
15. Claude, P., Hawrot, E., Dunis, D. A. & Campenot, R. B. *J. Neurosci.* **2,** 431–442 (1982).
16. Wayne, D. B. & Heaton, M. B. *Devl Biol.* **138,** 484–498 (1990).
17. Ernfors, P., Wetmore, C., Olson, L. & Persson, H. *Neuron* **5,** 511–526 (1990).
18. Schecterson, L. C. & Bothwell, M. *Neuron* **9,** 449–463 (1992).
19. Herzog, K. H., Bailey, K. & Barde, Y. A. *Development* **120,** 1643–1649 (1994).
20. Meakin, S. & Shooter, E. M. *Trends Neurosci.* **15,** 323–331 (1992).
21. Bothwell, M. *A. Rev. Neurosci.* **18,** 223–253 (1995).
22. von Bartheld, C. S., Heuer, J. G. & Bothwell, M. *J. comp. Neurol.* **310,** 103–129 (1991).
23. von Bartheld, C. S. *et al. Neuron* **12,** 639–654 (1994).
24. Smith, R. S., Hammerschlag, R., Snyder, R. E., Chan, H. & Bobinsky, J. *J. Neurochem.* **62,** 1698–1706 (1994).
25. Hammerschlag, R. & Stone, G. C. *Trends Neurosci.* **5,** 12–15 (1982).
26. Felder, S. *et al. Cell* **61,** 623–634 (1990).
27. Konrad, R. J. *et al. J. biol. Chem.* **270,** 12869–12876 (1995).
28. Williams, R., Bäckström, A., Kullander, K., Hallböök, F. & Ebendal, T. *Eur. J. Neurosci.* **7,** 116–128 (1995).
29. Richardson, P. M., Verge, V. M. K. & Riopelle, R. J. *J. Neurosci.* **6,** 2312–2321 (1986).
30. Byers, M. R. *Brain Res.* **75,** 97–113 (1974).
31. Zhou, X. F. & Rush, R. A. *Neuroscience* (in the press).

ACKNOWLEDGEMENTS. BDNF and NT-3 were kindly provided by Regeneron, bFGF by Chiron Corporation, and chicken BDNF and NT-3 DNA by P. Maisonpierre and G. Yancopoulos (Regeneron). We thank E. Gunther, R. Rush and X.-F. Zhou for sharing unpublished data; L. Schecterson for subcloning; S. Anderson and D. Cunningham for technical assistance; and Y. Barde, P. Clarke, E. Johnson, W. Mobley, R. Oppenheim, F. Peale, C. Shatz, H. Thoenen and L. Westrum for their comments. Our work was supported by grants from the NIH.

The inward rectification mechanism of the HERG cardiac potassium channel

Paula L. Smith, Thomas Baukrowitz & Gary Yellen*

Department of Neurobiology, Harvard Medical School and Massachusetts General Hospital, Boston, Massachusetts 02114-2698, USA

A HUMAN genetic defect associated with 'long Q–T syndrome', an abnormality of cardiac rhythm involving the repolarization of the action potential, was recently found to lie in the HERG gene, which codes for a potassium channel[1]. The HERG K^+ channel is unusual in that it seems to have the architectural plan of the depolarization-activated K^+ channel family (six putative transmembrane segments), yet it exhibits rectification like that of the inward-rectifying K^+ channels, a family with different molecular structure (two transmembrane segments)[2–4]. We have studied HERG channels expressed in mammalian cells and find that this inward rectification arises from a rapid and voltage-dependent inactivation process that reduces conductance at positive voltages. The inactivation gating mechanism resembles that of C-type inactivation, often considered to be the 'slow inactivation' mechanism of other K^+ channels. The characteristics of this gating suggest a specific role for this channel in the normal suppression of arrhythmias.

HERG K^+ channels expressed in mammalian cells have the same basic properties previously reported for channels expressed in oocytes[3,4]: they required depolarization for their activation, but they carried a relatively small outward current (Fig. 1*a*). On repolarization to a negative membrane potential, the conductance increased to a large value within a few milliseconds, before returning slowly to the resting closed state. The peak currents measured by stepping to various voltages after activation showed inward rectification (that is, the inward currents were substantially larger than the outward) (Fig. 1*b*). This inward rectification has been proposed to result from an 'inactivation' mechanism that turns channels off at positive potentials but quickly recovers at negative potentials[3–6], producing a rising phase in the inward current. Unlike the clear time-dependent inactivation of other voltage-activated K^+ channels like *Shaker*, this inactivation was thought to be kinetically invisible for depolarizing steps because it is much faster than activation.

The onset of this inactivation process was revealed by a modified voltage-clamp pulse protocol. After a long depolarizing pulse to activate the channels, the membrane was hyperpolarized

* To whom correspondence should be addressed at the Massachusetts General Hospital.

(Fig. 1*c*). Channels recovered rapidly from inactivation and then began to close slowly, but before they closed appreciably the membrane was again depolarized. At this time the channels were still activated (because they had not yet closed), but the inactivation process had to re-occur. This 're-inactivation' was seen as a single exponential decline in current, returning to the same steady-state level seen in the first depolarizing pulse.

Without this inactivation, the channels did not exhibit inward rectification. Channels were activated by depolarization and then hyperpolarized to −80 mV to allow them to recover from inactivation. From this starting point, an instantaneous current–voltage (*I–V*) relationship obtained by steps to varying voltages was roughly linear (Fig. 2*a*, *b*). This method measured the current through channels before inactivation gating was allowed to adjust to the new voltage. Thus, inactivation gating produces inward rectification in a channel with non-rectifying permeation properties.

We measured the steady-state voltage dependence of inactivation to see if it matched the voltage-dependent rectification. After a long depolarizing pulse to activate channels, the membrane voltage was stepped briefly to various test voltages and then to a constant measurement potential of +20 mV (Fig. 2*c*). During the brief step, the inactivation process relaxed rapidly to the steady-state level appropriate to the test potential. The initial current on stepping to +20 mV then gave the relative number of open channels, which was large at negative voltages that relieved inactivation, but smaller at more positive voltages where steady-state inactivation was significant. For very negative voltages, we corrected for the fast closing that occurred during the brief hyperpolarizing step (see Fig. 2 legend). The data could be fitted by a Boltzmann function with half inactivation at about −90 mV and an effective valence of about 1 (Fig. 2*d*).

If inward rectification results from this inactivation process, then the rectifying *I–V* should be given by the product of the open channel *I–V* (Fig. 2*b*) and the steady-state inactivation function (Fig. 2*d*). To test this, we re-plotted the peak *I–V* data of Fig. 1*a*, *b* with corrections at negative voltages for the de-activation process, and compared the rectification with the prediction (Fig. 2*e*). The match between the two shows that the inward rectification of HERG channels can be quantitatively accounted for by the properties of the inactivation process.

We then investigated the molecular basis of the HERG inactivation process. One mechanism for inward rectification used by some members of the inwardly rectifying K^+ channel family, is a voltage-dependent channel blockade by intracellular Mg^{2+} (refs 7–10). If the onset of this blockade were sufficiently slow, it could appear as a time-dependent inactivation process. But we found that Mg^{2+} did not play a role in HERG inactivation. The presence or absence of Mg^{2+} in the intracellular solution perfusing an excised inside-out patch made no difference in the rate or extent of inactivation (Fig. 3*a*).

Inactivation of another voltage-activated K^+ channel, the *Shaker* K^+ channel from *Drosophila*, occurs by two distinct molecular mechanisms: N-type inactivation, which occurs by an intracellular ball-and-chain mechanism[11–13], and C-type inactivation, which involves a conformational change at the outer mouth of the channel[14–16]. The classical K^+ channel blocker tetraethylammonium (TEA) can be used to distinguish the two mechanisms: blockade by intracellular TEA inhibits N-type inactivation, whereas blockade by extracellular TEA inhibits C-type inactivation[15].

We tested the effects of TEA on the HERG inactivation process. Intracellular TEA applied to an inside-out patch reduced the HERG current with an apparent affinity of about 0.2 mM, but there was no change in the time course of inactivation (Fig. 3*b*). This effectively ruled out an N-type inactivation mechanism, and indeed any mechanism that relies on an intracellular pore blocker. Any such mechanism should compete with the binding of TEA to the intracellular mouth, and it would thus be slower in the presence of TEA.

By contrast, extracellular TEA did interfere with inactivation. Extracellular application of 100 mM TEA reduced the peak current and slowed the time course of inactivation (Fig. 3*c*). The simplest explanation for this combination of effects, which is also seen for the C-type inactivation mechanism of *Shaker* channels[15], is that blocked channels (B) cannot inactivate (I) (O, open):

$$B \underset{K_{on}\cdot[TEA]}{\overset{k_{off}}{\rightleftharpoons}} O \overset{\alpha}{\rightharpoonup} I$$

If binding and dissociation of the blocker are rapid (at equilibrium) relative to the rate of inactivation (α), then the apparent rate

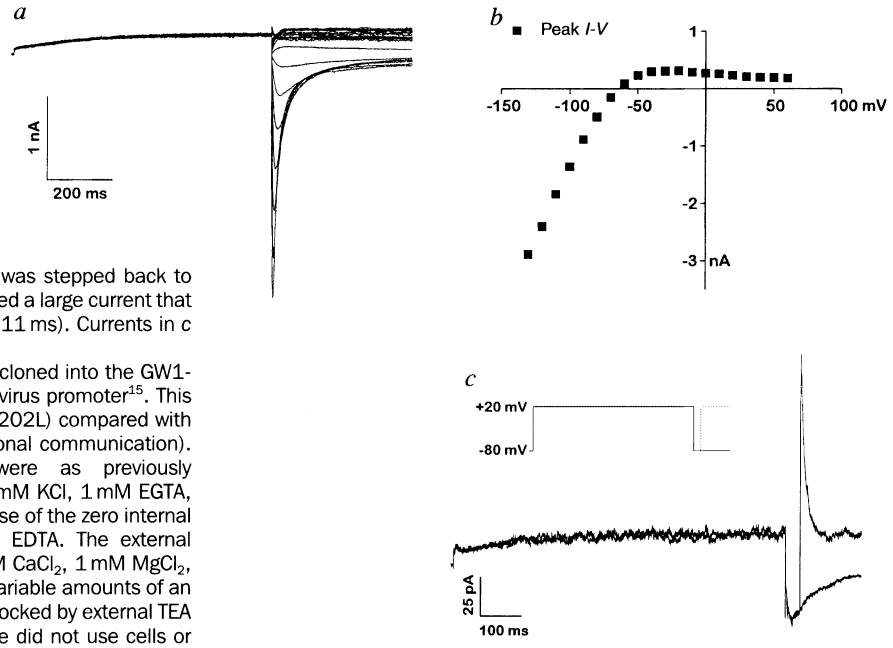

FIG. 1 Inward rectification of HERG and the HERG inactivation process. *a*, HERG currents transiently expressed in an HEK293 cell were activated by a long depolarizing pulse to +20 mV, and then stepped to various voltages to show inward rectification. *b*, Peak *I–V* from the currents in *a*. *c*, Method used to show the onset of HERG inactivation. After a long step to +20 mV to activate the channels, repolarization to −80 mV produced rapid recovery from inactivation. If the voltage was maintained at −80 mV, channels proceeded to close by de-activation. If the voltage was stepped back to +20 mV after 30 ms, the recovered channels produced a large current that then declined through the inactivation process ($\tau \sim 11$ ms). Currents in *c* were measured from an excised outside-out patch.

METHODS. The HERG complementary DNA was subcloned into the GW1-CMV vector under control of the human cytomegalovirus promoter[15]. This cDNA contained two point mutations (V198E and P202L) compared with the published HERG sequence (G. Robertson, personal communication). Transfection and electrophysiology methods were as previously described[22,24]. The basic internal solution was 160 mM KCl, 1 mM EGTA, 0.5 mM $MgCl_2$, 10 mM HEPES, pH 7.4 and in the case of the zero internal Mg^{2+} experiments, $MgCl_2$ was replaced by 5 mM EDTA. The external solution contained 150 mM NaCl, 10 mM KCl, 3 mM $CaCl_2$, 1 mM $MgCl_2$, 10 mM HEPES, pH 7.4. The HEK293 cells express variable amounts of an endogenous outward rectifier K^+ channel, which is blocked by external TEA with an affinity of about 1 mM (data not shown). We did not use cells or patches where the endogenous current was substantial compared with HERG expression.

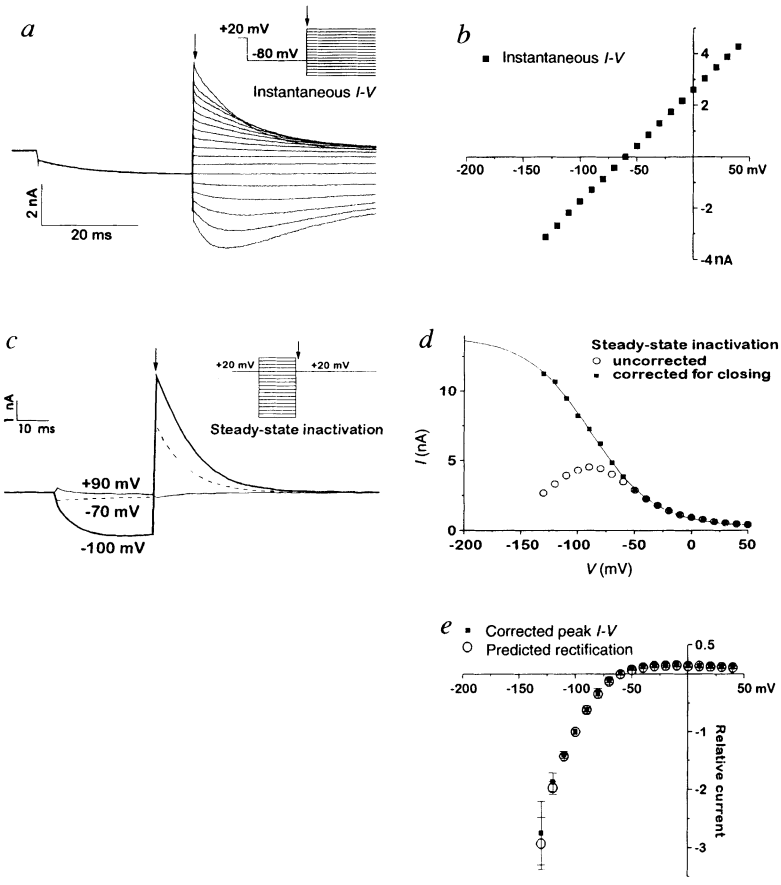

FIG. 2 The inactivation process accounted for inward rectification. *a*, An instantaneous *I–V* protocol showed that the open-channel *I–V*, before the onset of inactivation, was linear. *b*, Plot of the instantaneous *I–V* measured at the time of the arrow in *a*. *c*, Method used to assess steady-state inactivation. After allowing inactivation to relax to steady state at various voltages, the membrane voltage was stepped to +20 mV to assess the relative number of channels available to activate. *d*, Steady-state inactivation from *c*. The initial current (arrow in *c*) was plotted as a function of the previous voltage step (○). At negative voltages, the currents declined because significant closing of channels occurred through de-activation. This was corrected for by extrapolating the exponential falling phase (measured in full at the end of the procedure, but not shown; see Fig. 1*a*) back to the start of the negative voltage step, and applying the same relative correction to the initial outward current. The corrected inactivation curve (■) was well-fitted by a Boltzmann function (solid line) with a voltage midpoint of −90 ± 6 mV and an effective valence of −1.0 ± 0.1. *e*, Comparison between the measured inward rectification and the rectification predicted from the inactivation curve. Inward rectification (■) was measured as in Fig. 1*b* and then corrected for closing at negative voltages (as in *d*). The prediction was made by multiplying the instantaneous *I–V* (from *b*) by the inactivation function (from *d*). Values from three experiments were normalized to equal one at −100 mV and then averaged; the error bars indicate the s.e.m.

METHODS. Back-extrapolation of the closing phase may not be precisely correct if inactivated channels do not close at the same rate. Nevertheless we think that the error was small as fits constrained only by the uncorrected data in the voltage range −80 to +40 gave roughly the same parameters.

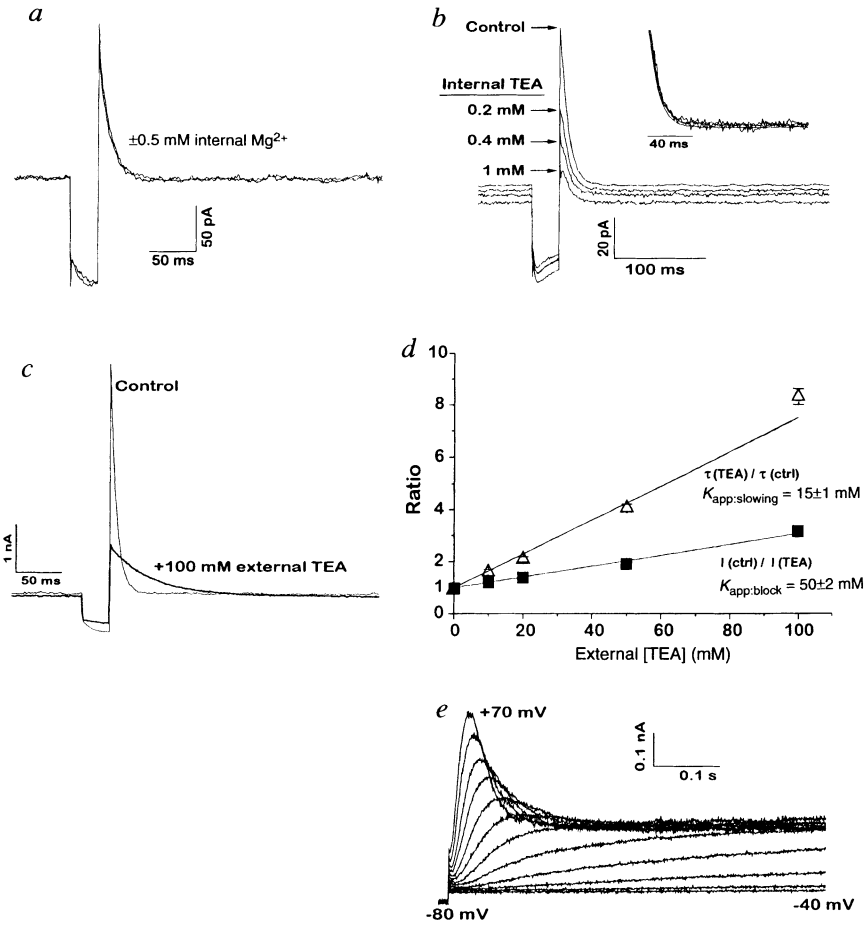

FIG. 3 Effects of Mg^{2+} ions and TEA on the HERG inactivation process. *a*, HERG currents from an inside-out patch perfused with 0.5 mM Mg^{2+} or with 5 mM EDTA. The initial voltage was +20 mV, followed by a 30-ms pulse to −80 mV, with re-inactivation at +20 mV. *b*, HERG currents from an inside-out patch perfused with various concentrations of internal TEA. Voltage steps as in *a*. The horizontal arrows indicate the initial peaks, which declined as internal TEA was raised. All currents inactivated with a time constant of about 9 ms. If the currents were normalized at the peak, they superimposed (inset). *c*, External TEA blocked the peak current and slowed inactivation. Voltage steps as in *a*. *d*, Effect of external TEA on the time constant of inactivation (△) and on the peak initial current at +20 mV (■). In each case, the fold-change was plotted against [TEA]. $K_{apparent}$ for TEA in each case was given by the reciprocal of the slope. Mean and range of two experiments. *e*, Activating voltage family in the presence of 100 mM external TEA. At positive voltages, activation was faster than the inactivation (which had been slowed by the TEA).

METHODS. The intrinsic voltage dependence of TEA blockage was small or nonexistent (data not shown). If it were large, the relationship in the text would not be correct, because the redistribution between gating states would occur at −80 mV but the blockade would be measured finally at +20 mV.

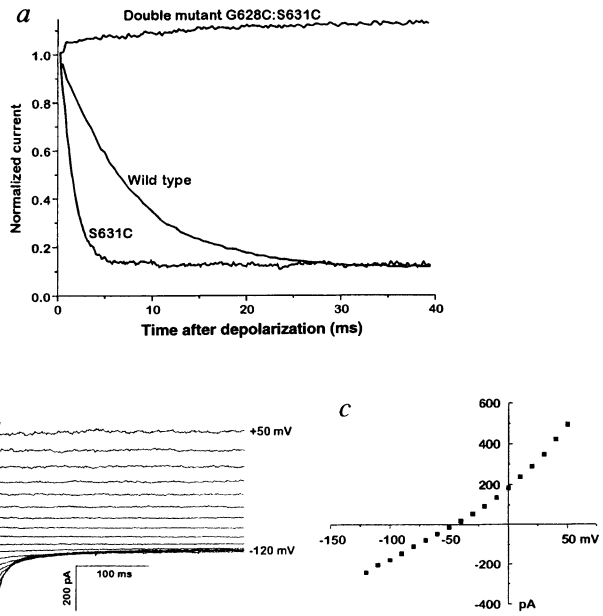

FIG. 4 Effects of two pore mutations on HERG inactivation. *a*, Comparison of inactivation for wild-type HERG channels and the mutant channels S631C and G628C:S631C. Inactivation was observed at +20 mV using methods like those in Fig. 3. For wild type, the preceding step to −80 mV lasted 35 ms; for the mutants, it was 15 ms. *b*, Absence of inward rectification in the HERG double mutant G628C:S631C, using the method of Fig. 1*b*. Dotted line indicates zero current level. *c*, *I–V* relationship for the double mutant, measured at the time indicated by the arrow in *b*.

of inactivation will be

$$\alpha_{app} = \alpha \cdot \left[\frac{O}{O+B}\right] = \alpha \cdot \left[\frac{1}{1+[TEA]/K_d}\right]$$

where $K_d = k_{off}/k_{on}$ and the time constant for inactivation in TEA (assuming that recovery is much slower than onset) is $\tau_{TEA} = \tau_{ctrl} \cdot (1 + [TEA]/K_d)$, where $\tau_{ctrl} = \alpha^{-1}$. Plotting τ_{TEA}/τ_{ctrl} as a function of [TEA] gave this straight-line relationship (Fig. 3*d*), with a K_d value of 15 ± 1 mM.

We compared this with the affinity estimated from current inhibition. A simple plot of current reduction as a function of [TEA] gave a much lower apparent affinity of 50 ± 2 mM (Fig. 3*d*), but this measurement was tainted by the interaction between TEA and inactivation. In the presence of TEA, channels equilibrate during the prepulse to −80 mV among three states—open, blocked and inactivated—and the redistribution of channels from the inactivated state reduces the apparent blockade. The apparent affinity measured under these conditions should be $K_{app} = K_d \cdot (1 + K_I)$, where K_d is the true dissociation constant and K_I is the equilibrium constant for inactivation at −80 mV. From the steady-state inactivation measurement of Fig. 2*c*, $K_I = 1.7 \pm 0.5$, and the true K_d estimated from the current inhibition was 19 ± 4 mM, in reasonable agreement with the K_d for the slowing of inactivation.

Because TEA slows the effective rate of HERG inactivation, it can be used as an alternative tool for separating the two gating processes. In the presence of TEA, and particularly at very positive voltages, activation became faster than inactivation and the outward HERG current resembled that of a 'normal' voltage-activated channel like *Shaker*: rapid voltage-dependent activation is followed by inactivation (Fig. 3*e*). This finding supports a coherent picture of HERG as a member of the voltage-activated K^+ channel family, with an unusually slow activation and fast inactivation process. This may be different from the KAT1 K^+ channel (the other known inward rectifier with 6 transmembrane segments), in which rectification is proposed to result from a voltage-activation mechanism with reversed polarity[17–19].

To explore further the relationship between HERG inactivation and *Shaker* C-type inactivation, we made mutations in the outer mouth of the HERG channel at position 631. This residue is homologous to position 449 in the outer mouth of *Shaker* channels, which has large effects on C-type inactivation[16,20]. In HERG, mutating this position from serine to cysteine (S631C) produced a substantial increase in the rate of inactivation (Fig. 4*a*). Voltage-dependent activation and de-activation of the channel remained slow. By accident, our mutagenesis procedure also produced a double mutant (G628C:S631C) with very interesting properties: it lacked the normal HERG inactivation completely. The double mutant showed no inactivation (Fig. 4*a*), and it lacked inward rectification (Fig. 4*b*, *c*). The instantaneous *I–V* reversed at a more positive voltage than the wild type, indicating a reduced selectivity for K^+ as is seen for mutations at the homologous position in *Shaker*[21].

The single mutant G628C did not express, and we do not know the mechanism by which the two mutations in the double mutant interact to produce a functional channel that lacks inactivation. Nevertheless, the dramatic effects of pore mutations on the HERG inactivation process are consistent with the idea that it may be mechanistically similar to C-type inactivation of *Shaker* channels. The HERG inactivation process seems to be much faster and more voltage-dependent than *Shaker* C-type inactivation, but the rate and voltage dependence of *Shaker* inactivation can vary with mutation and ionic conditions[20,22,23]. Thus it seems possible that the main differences between the two processes are quantitative and not qualitative.

The mechanism of rectification has important implications for the pharmacology of HERG and its *in vivo* equivalent (I_{Kr}), as blockers acting at the inner and outer mouths of the channel will interact differently with the inactivation process. Also, the kinetics of HERG inactivation indicate that these channels may be important in the normal physiological suppression of arrhythmias, specifically in suppressing the generation of premature afterbeats. The conditions under which we produced large outward (inhibitory) currents through these channels, prompt re-activation (Fig. 1*c*), are like those that occur during generation of a premature beat. Such a role for HERG in suppressing extra beats might help to explain the increased incidence of cardiac sudden death in patients that lack HERG currents, either because they carry a genetic defect (familial long QT syndrome) or because they are being treated with class III antiarrhythmics that block HERG channels. □

Received 24 November 1995; accepted 4 January 1996.

1. Curran, M. E. *et al. Cell* **80,** 795–803 (1995).
2. Warmke, J. W. & Ganetzky, B. *Proc. natn. Acad. Sci. U.S.A.* **91,** 3438–3442 (1994).
3. Sanguinetti, M. C., Jiang, C., Curran, M. E. & Keating, M. T. *Cell* **81,** 299–307 (1995).
4. Trudeau, M. C., Warmke, J. W., Ganetzky, B. & Robertson, G. A. *Science* **269,** 92–95 (1995).
5. Sanguinetti, M. C. & Jurkiewicz, N. K. *J. gen. Physiol.* **96,** 195–215 (1990).
6. Shibasaki, T. *J. Physiol., Lond.* **387,** 227–250 (1987).
7. Vandenberg, C. A. *Proc. natn. Acad. Sci. U.S.A.* **84,** 2560–2564 (1987).
8. Lu, Z. & MacKinnon, R. *Nature* **371,** 243–246 (1994).
9. Nichols, C. G., Ho, K. & Hebert, S. *J. Physiol., Lond.* **476,** 399–409 (1994).
10. Stanfield, P. R. *et al. J. Physiol., Lond.* **475,** 1–7 (1994).
11. Hoshi, T., Zagotta, W. N. & Aldrich, R. W. *Science* **250,** 533–538 (1990).
12. Zagotta, W. N., Hoshi, T. & Aldrich, R. W. *Science* **250,** 568–571 (1990).
13. Demo, S. D. & Yellen, G. *Neuron* **7,** 743–753 (1991).
14. Hoshi, T., Zagotta, W. N. & Aldrich, R. W. *Neuron* **7,** 547–556 (1991).
15. Choi, K. L., Aldrich, R. W. & Yellen, G. *Proc. natn. Acad. Sci. U.S.A.* **88,** 5092–5095 (1991).
16. Yellen, G., Sodickson, D., Chen, T.-Y. & Jurman, M. E. *Biophys. J.* **66,** 1068–1075 (1994).
17. Anderson, J. A., Huprikar, S. S., Kochian, L. V., Lucas, W. J. & Gaber, R. F. *Proc. natn. Acad. Sci. U.S.A.* **89,** 3736–3740 (1992).
18. Cao, Y., Crawford, N. M. & Schroeder, J. I. *J. biol. Chem.* **270,** 17697–17701 (1995).
19. Hoshi, T. *J. gen. Physiol.* **105,** 309–328 (1995).
20. López-Barneo, J., Hoshi, T., Heinemann, S. H. & Aldrich, R. W. *Recept. Chan.* **1,** 61–71 (1993).
21. Heginbotham, L., Lu, Z., Abramson, T. & MacKinnon, R. *Biophys. J* **66,** 1061–1067 (1994).
22. Baukrowitz, T. & Yellen, G. *Neuron* **15,** 951–960 (1995).
23. Baukrowitz, T. & Yellen, G. *Science* **271,** 653–656 (1996).
24. Jurman, M. E., Boland, L. M., Liu, Y. & Yellen, G. *BioTechniques* **17,** 876–881 (1994).

ACKNOWLEDGEMENTS. We thank M. Jurman for assistance in preparing the mutants and the transfected cells, and G. Robertson for the cDNA clone for HERG. This work was partially supported by the National Institute of Neurological Diseases and Stroke (to G.Y.), by a Gottlieb Daimler–Karl Benz stipend (T.B.), and by an NIH training grant (P.L.S.).